Supporting information

EPS inhibitor treatment of *Salmonella* impacts evolution without selecting for resistance to biofilm inhibition

Mathieu Joos[1,†], Sybren Van Ginneken[1,†], Xabier Villanueva[1], Marie Dijkmans[1], Guglielmo A. Coppola[1,2], Camilo Andres Pérez-Romero[3], Thijs Vackier[1], Erik Van der Eycken[2,4], Kathleen Marchal[3], Bram Lories[1,#] & Hans P. Steenackers[1,#,*]

[1] KU Leuven - MiCA Lab, Centre of Microbial and Plant Genetics, Leuven, Belgium

[2] KU Leuven - Laboratory for Organic & Microwave-Assisted Chemistry (LOMAC), Department of Chemistry, Leuven, Belgium

[3] UGent – Internet technology and Data science Lab (IDLab), Department of Plant Biotechnology and Bioinformatics, Gent, Belgium

[4] People's Friendship University of Russia (RUDN University) – Miklukho-Maklaya street 6, Moscow, Russia

*** Correspondence:**
Hans P. Steenackers
hans.steenackers@kuleuven.be

† These authors contributed equally to this work.

These authors share last authorship

Supplementary Figures & Tables

Supplementary Table 1 Primers used for RT-qPCR analysis. Primers used for RT-qPCR analysis of *csgD* expression. See Material and Methods section for experimental details.

Gene	Forward primer	Reverse primer	Reference
csgD *(biofilm regulator)*	5'-TGTCTTAACCGTATTCTCGCTGAT-3'	5'-AGCACCGAGTCCGCATTACT-3'	ca
rpoD *(housekeeping)*	5'-TTCCAGCAGATAGGTAATGGCTTC-3'	5'-GTGAAATGGGCACTGTTGAACTG-3'	2
rfaH *(housekeeping)*	5'-AAACGCGGGCAACTTCAG-3'	5'-GTCAGGCAACTTACCGCTTGT-3'	3
16s rDNA *(housekeeping)*	5'-CGGGGAGGAAGGTGTTGTG-3'	5'-GAGCCCGGGGATTTCACATC-3'	4

Supplementary Table 2 Clones recovered from the RC41-evolved populations show abolished catalase activity. From each end-point evolved population, 20 *Salmonella* Typhimurium ATCC14028 clones were randomly picked and functionality of their σ^S regulon was qualitatively assessed using a catalase assay. Between 5 and 20% of the tested clones failed to show catalase activity, which roughly corresponds with the observed frequencies of *rpoS* and *rpoC* mutations in each population. Clones recovered from control-evolved populations all showed catalase activity. For the clones that did not show catalase activity, the *rpoS* and *rpoC* genes were Sanger sequenced and identified mutations are shown.

Population	Mutation identified in populations (see Table 1)		Clones without catalase activity (n=20)	Colony n°	Mutations identified in clones	
	rpoS	*rpoC*			*rpoS*	*rpoC*
RC41-1	/	Leu363Pro (29%)	15%	7	/	Leu363Pro
		His450Tyr (25%)		11	/	Leu363Pro
		Arg481Cys (21%)		12	/	Leu363Pro
RC41-2	Asp37fs (11%)	/	5%	16	/	/
RC41-3	Trp149Arg (18%)	/	20%	4	Trp149Arg	/
				5	Trp149Arg	/
	Asp37fs (16%)			8	Trp149Arg	/
				20	Trp149Arg	/

Supplementary Table 3 *p*-values of the statistical comparison of growth rates displayed in Figure 5. Planktonic growth of wild-type (WT) *Salmonella* Typhimurium ATCC14028 and end-point evolved populations was measured in the presence or absence of 50 µM of the 2-AI-based EPS inhibitor (RC41). A *ramR* and *rpoS* deletion construct (Δ*ramR* & Δ*rpoS*) and a double deletion construct (Δ*ramR*Δ*rpoS*) were included as references. Growth curves are shown in **Figure 5** and **Supplementary Figure 6**. Growth rates (OD_{600nm} h^{-1}) were extracted from growth curves by fitting a Zwietering-modified Gompertz model and are shown in **Figure 5**. Significant differences between growth rates were tested using a two-way ANOVA, followed by Tukey's multiple comparisons test. All *p*-values are shown in the table below.

Sample 1		**Sample 2**		***p*-value**
Population	**Treatment**	**Population**	**Treatment**	
WT	0 µM	WT	50 µM	<0.0001
Control-evolved	0 µM	Control-evolved	50 µM	<0.0001
RC41-evolved	0 µM	RC41-evolved	50 µM	0.3550
Δ*ramR*	0 µM	Δ*ramR*	50 µM	<0.0001
Δ*rpoS*	0 µM	Δ*rpoS*	50 µM	0.0006
Δ*ramR*Δ*rpoS*	0 µM	Δ*ramR*Δ*rpoS*	50 µM	<0.0001
WT	0 µM	Control-evolved	0 µM	0.9384
WT	0 µM	RC41-evolved	0 µM	0.2184
WT	0 µM	Δ*ramR*	0 µM	0.9986
WT	0 µM	Δ*rpoS*	0 µM	>0.9999
WT	0 µM	Δ*ramR*Δ*rpoS*	0 µM	0.9175
Control-evolved	0 µM	RC41-evolved	0 µM	0.7196
Control-evolved	0 µM	Δ*ramR*	0 µM	0.9947
Control-evolved	0 µM	Δ*rpoS*	0 µM	0.9428
Control-evolved	0 µM	Δ*ramR*Δ*rpoS*	0 µM	0.3857
RC41-evolved	0 µM	Δ*ramR*	0 µM	0.4041
RC41-evolved	0 µM	Δ*rpoS*	0 µM	0.2249
RC41-evolved	0 µM	Δ*ramR*Δ*rpoS*	0 µM	0.0198
Δ*ramR*	0 µM	Δ*rpoS*	0 µM	0.9989
Δ*ramR*	0 µM	Δ*ramR*Δ*rpoS*	0 µM	0.7211
Δ*rpoS*	0 µM	Δ*ramR*Δ*rpoS*	0 µM	0.9116
WT	50 µM	Control-evolved	50 µM	0.9983
WT	50 µM	RC41-evolved	50 µM	0.0160
WT	50 µM	Δ*ramR*	50 µM	0.7044
WT	50 µM	Δ*rpoS*	50 µM	0.0669
WT	50 µM	Δ*ramR*Δ*rpoS*	50 µM	0.4494
Control-evolved	50 µM	RC41-evolved	50 µM	0.0058
Control-evolved	50 µM	Δ*ramR*	50 µM	0.4525
Control-evolved	50 µM	Δ*rpoS*	50 µM	0.0267
Control-evolved	50 µM	Δ*ramR*Δ*rpoS*	50 µM	0.2304
RC41-evolved	50 µM	Δ*ramR*	50 µM	0.3029
RC41-evolved	50 µM	Δ*rpoS*	50 µM	0.9875
RC41-evolved	50 µM	Δ*ramR*Δ*rpoS*	50 µM	0.3913
Δ*ramR*	50 µM	Δ*rpoS*	50 µM	0.6674
Δ*ramR*	50 µM	Δ*ramR*Δ*rpoS*	50 µM	0.9995
Δ*rpoS*	50 µM	Δ*ramR*Δ*rpoS*	50 µM	0.7909

Supplementary Table 4 *p*-values of the statistical comparison of lag times displayed in Figure 5. Planktonic growth of wild-type (WT) *Salmonella* Typhimurium ATCC14028 and end-point evolved populations was measured in the presence or absence of 50 µM of the 2-AI-based EPS inhibitor (RC41). A *ramR* and *rpoS* deletion construct (Δ*ramR* & Δ*rpoS*) and a double deletion construct (Δ*ramR*Δ*rpoS*) were included as references. Growth curves are shown in **Figure 5** and **Supplementary Figure 6**. Lag times (h) were extracted from growth curves by fitting a Zwietering-modified Gompertz model and are shown in **Figure 5**. Significant differences between lag times were tested using a two-way ANOVA, followed by Tukey's multiple comparisons test. All *p*-values are shown in the table below.

Sample 1		**Sample 2**		***p*-value**
Population	**Treatment**	**Population**	**Treatment**	
WT	0 µM	WT	50 µM	<0.0001
Control-evolved	0 µM	Control-evolved	50 µM	<0.0001
RC41-evolved	0 µM	RC41-evolved	50 µM	0.0349
Δ*ramR*	0 µM	Δ*ramR*	50 µM	0.0011
Δ*rpoS*	0 µM	Δ*rpoS*	50 µM	<0.0001
Δ*ramR*Δ*rpoS*	0 µM	Δ*ramR*Δ*rpoS*	50 µM	0.0900
WT	0 µM	Control-evolved	0 µM	0.9985
WT	0 µM	RC41-evolved	0 µM	0.6081
WT	0 µM	Δ*ramR*	0 µM	0.9996
WT	0 µM	Δ*rpoS*	0 µM	>0.9999
WT	0 µM	Δ*ramR*Δ*rpoS*	0 µM	0.0700
Control-evolved	0 µM	RC41-evolved	0 µM	0.8781
Control-evolved	0 µM	Δ*ramR*	0 µM	>0.9999
Control-evolved	0 µM	Δ*rpoS*	0 µM	0.9994
Control-evolved	0 µM	Δ*ramR*Δ*rpoS*	0 µM	0.0212
RC41-evolved	0 µM	Δ*ramR*	0 µM	0.7827
RC41-evolved	0 µM	Δ*rpoS*	0 µM	0.7074
RC41-evolved	0 µM	Δ*ramR*Δ*rpoS*	0 µM	0.0012
Δ*ramR*	0 µM	Δ*rpoS*	0 µM	>0.9999
Δ*ramR*	0 µM	Δ*ramR*Δ*rpoS*	0 µM	0.0349
Δ*rpoS*	0 µM	Δ*ramR*Δ*rpoS*	0 µM	0.0480
WT	50 µM	Control-evolved	50 µM	0.9463
WT	50 µM	RC41-evolved	50 µM	0.0012
WT	50 µM	Δ*ramR*	50 µM	0.4383
WT	50 µM	Δ*rpoS*	50 µM	0.1455
WT	50 µM	Δ*ramR*Δ*rpoS*	50 µM	0.8954
Control-evolved	50 µM	RC41-evolved	50 µM	0.0001
Control-evolved	50 µM	Δ*ramR*	50 µM	0.0964
Control-evolved	50 µM	Δ*rpoS*	50 µM	0.5646
Control-evolved	50 µM	Δ*ramR*Δ*rpoS*	50 µM	0.3690
RC41-evolved	50 µM	Δ*ramR*	50 µM	0.1026
RC41-evolved	50 µM	Δ*rpoS*	50 µM	<0.0001
RC41-evolved	50 µM	Δ*ramR*Δ*rpoS*	50 µM	0.0076
Δ*ramR*	50 µM	Δ*rpoS*	50 µM	0.0019
Δ*ramR*	50 µM	Δ*ramR*Δ*rpoS*	50 µM	0.9284
Δ*rpoS*	50 µM	Δ*ramR*Δ*rpoS*	50 µM	0.0096

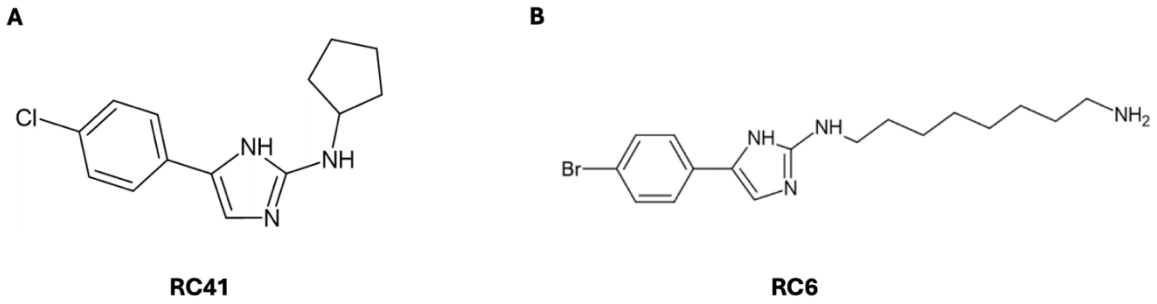

Supplementary Figure 1 Chemical structure of the EPS inhibitors. Chemical structure of the 2-amino-imidazole-based EPS inhibitors RC41 (**A**) and RC6 (**B**).

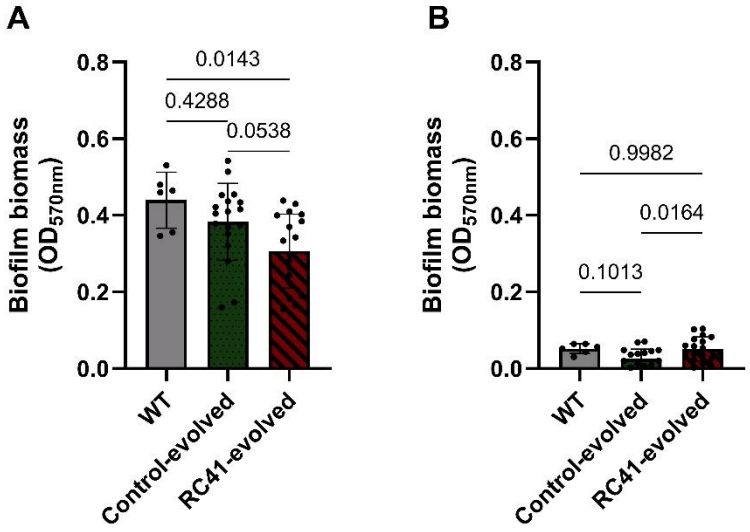

Supplementary Figure 2 Biofilm biomass of single clones isolated from the evolved populations. In addition to the population-level measurements, we also isolated single clones of *Salmonella* Typhimurium ATCC14028 from each of the end-point evolved populations and quantified the biofilm biomass in the absence (**A**) and presence (**B**) of the 2-AI-based EPS inhibitor RC41. Each datapoint represents a single clone isolated from the indicated population. Bars represent the mean and error bars represent the standard deviation. Significant differences were tested using an ordinary one-way ANOVA, followed by Tukey's multiple comparisons test. All *p*-values are shown.

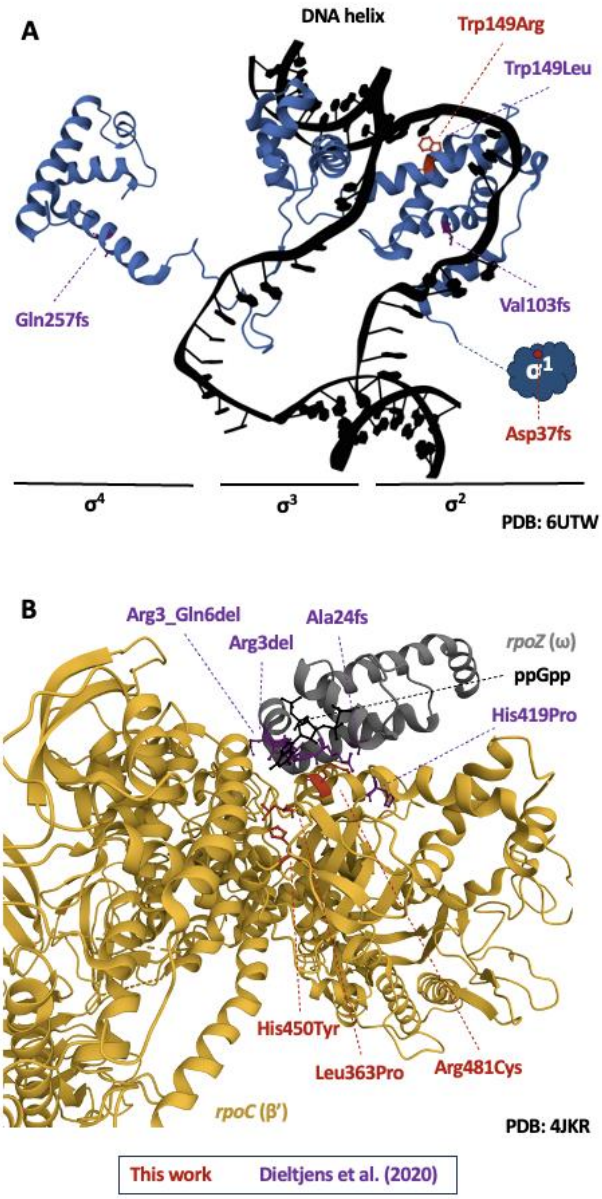

Supplementary Figure 3 *Salmonella* biofilm populations previously treated with RC41 by Dieltjens et al. (2020) show similar mutations in the RNA polymerase complex. During previous work[5], three independent S. Typhimurium ATCC14028 biofilms were repeatedly exposed to the 2-AI-based EPS inhibitor RC41. End-point population samples stored at -80°C were subjected to whole-genome sequencing. Similar to the biofilms evolved in this work, previously evolved populations show mutations in the RNA polymerase complex. In all three previously evolved populations, mutations (Val103fs, Trp149Leu, Gln257fs) mapping to *rpoS*, which encodes the stationary phase sigma factor σ^S, are found (**A**). Similar to the mutations observed in this work, they likely correspond to a σ^S loss-of-function. The *Escherichia coli* σ^S crystal structure was retrieved from PDB 6UTW[6]. In addition to *rpoS* mutations, mutations mapping to the ppGpp binding pocket were also observed in the previously evolved populations (**B**). While some of these mutations (His419Pro) map to the *rpoC* gene, which encodes the β' subunit of the RNA polymerase complex, most of the mutations (Arg3del, Arg3_Gln6del, Ala24fs) map to *rpoZ*, which encodes the ω subunit. The crystal structure of the *E. coli* RNA polymerase in complex with ppGpp was retrieved from PDB 4JKR[7]. Mutations observed in the biofilms evolved in this study are indicated in red, while mutations observed in the populations evolved by Dieltjens et al. (2020) are indicated in purple.

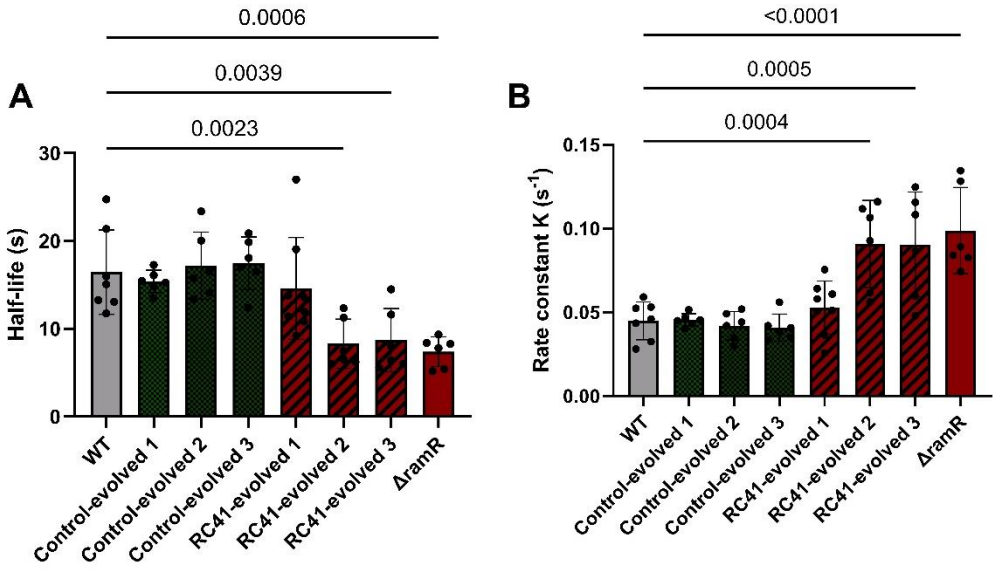

Supplementary Figure 4 Two out of three RC41-evolved populations show elevated efflux levels. Efflux of the evolved *Salmonella* Typhimurium ATCC14028 populations was quantified by measuring the decay in fluorescence of cells loaded with the periplasmic dye Nile Red. A one-step exponential decay model was fit, and the half-life (**A**) and rate constant (K; **B**) of the fluorescent decay were estimated. Each datapoint represents a biological repeat (n= 6-8). Bars represent the mean and error bars represent the standard deviation. Significant differences between the wild-type *Salmonella* and the evolved populations were tested using an ordinary one-way ANOVA, followed by Dunnett's multiple comparison test. For all significant differences, *p*-values are shown.

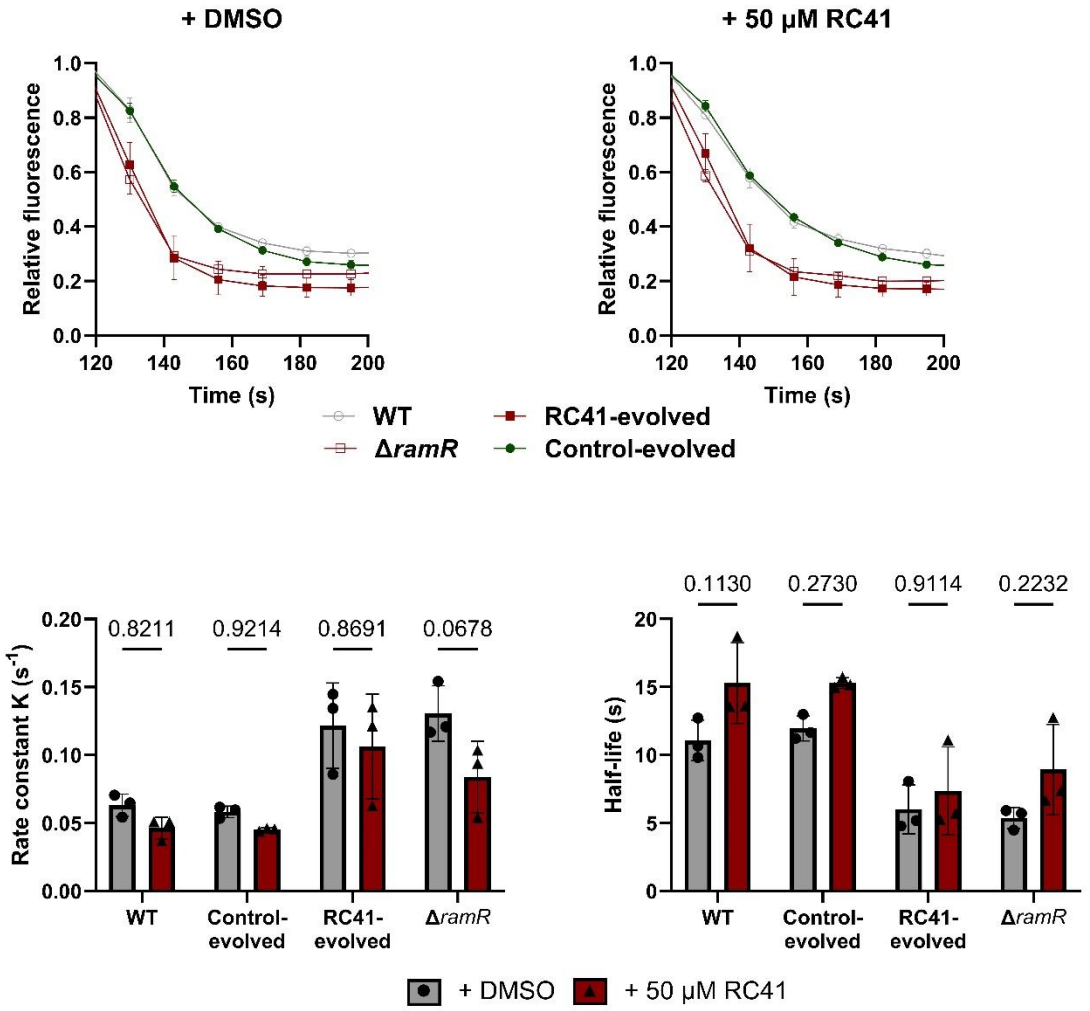

Supplementary Figure 5 RC41 does not affect efflux levels during short-term exposure. Efflux of wild-type (WT) *Salmonella* Typhimurium ATCC14028, an isogenic *ramR* deletion construct (Δ*ramR*) and the evolved biofilm populations was quantified by measuring the decay in fluorescence of cells loaded with the periplasmic dye Nile Red. Efflux was measured in the presence of either 50 µM of the 2-AI-based EPS inhibitor RC41 or the carrier solvent (DMSO) alone. A one-step exponential decay model was fit, and the half-life and rate constant (K) of the fluorescent decay were estimated. For WT *Salmonella* and the Δ*ramR* construct, each datapoint represents a biological repeat (n= 3). For the evolved populations, each datapoint represents an independently evolved lineage, for which the average of three replicates is shown (n= 3). Bars represent the mean and error bars represent the standard deviation. For the relative fluorescence vs time graph, each datapoint represents an average value and standard deviations are shown as error bars. Significant differences between the treated and untreated samples were tested using a two-way ANOVA, followed by Sidak's multiple comparison test. All *p*-values are shown.

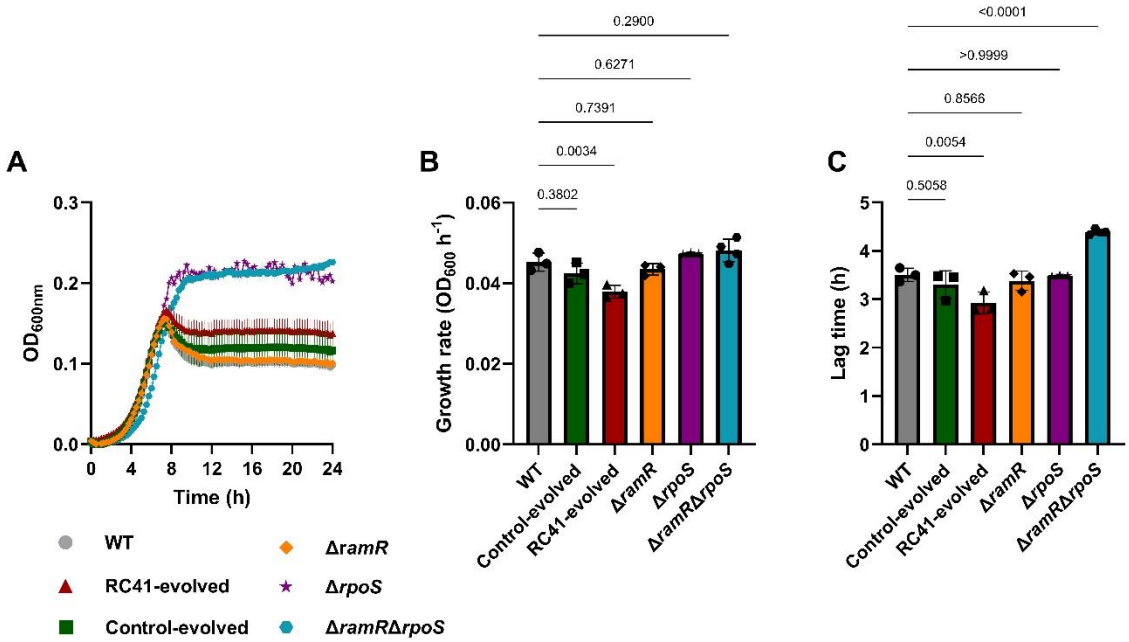

Supplementary Figure 6 Growth characteristics of the evolved populations in the absence of RC41 treatment. (**A**) Planktonic growth of wild-type (WT) *Salmonella* Typhimurium ATCC14028 and end-point evolved populations was measured in the absence of any EPS inhibitor. A *ramR* deletion construct (Δ*ramR*), an *rpoS* deletion construct (Δ*rpoS*), and a double deletion construct (Δ*ramR*Δ*rpoS*) were included as references. Growth rates (OD_{600nm} h^{-1}) and lag times (h) were extracted from growth curves by fitting a Zwietering-modified Gompertz model (**B**,**C**). For the wild-type, Δ*ramR*, Δ*rpoS* and Δ*ramR*Δ*rpoS* strains, each datapoint represents a biological repeat (n= 3-4). For the evolved populations, each datapoint represents an independently evolved lineage, for which the average of three replicates is shown (n= 3). Lines and bars represent the mean and error bars represent the standard deviation. Significance was tested relative to the wild-type using a one-way ANOVA, followed by Dunnett's multiple comparisons test. All *p*-values are shown.

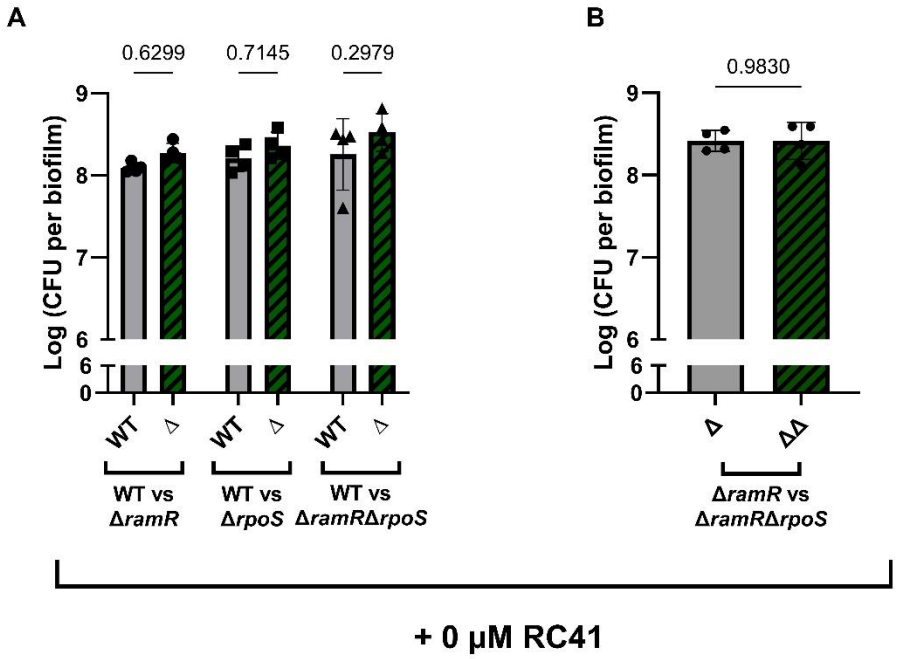

Supplementary Figure 7 Biofilm competition experiments in the absence of any EPS inhibitor. Biofilm competition experiments in small Petri-dishes were performed between wild-type (WT) *Salmonella* Typhimurium ATCC14028 and isogenic deletion constructs (Δ*ramR*, Δ*rpoS*, Δ*ramR*Δ*rpoS*) (**A**), or between the Δ*ramR* and Δ*ramR*Δ*rpoS* construct (**B**). Biofilms were inoculated in a 1:1 ratio and only treated with the carrier solvent (DMSO). After 48h of incubation, biofilms were scraped off and both competitors were quantified by counting Colony Forming Units (CFU). Each datapoint represents a biological repeat (n= 4). Bars represent the mean, while error bars represent the standard deviation. Significant differences in cell counts between both competitors were tested using a two-way ANOVA, followed by Sidak's multiple comparisons test (**A**), or a paired, two-tailed Student's t-test (**B**). All *p*-values are shown.

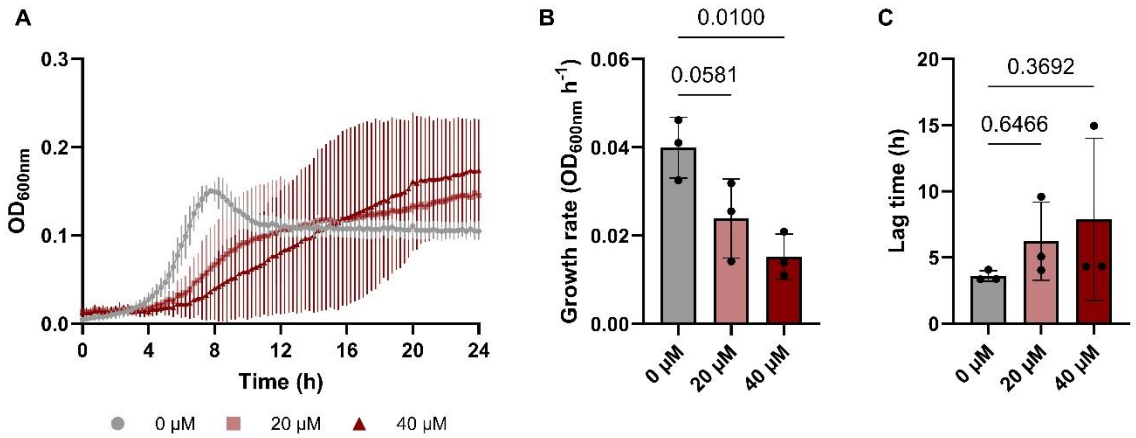

Supplementary Figure 8 Lower concentrations of RC41 still delay planktonic growth. (**A**) Planktonic growth of wild-type *Salmonella* Typhimurium ATCC14028 was measured in the presence of the 2-AI-based EPS inhibitor RC41 (0 µM, 20 µM, 40 µM). Growth rates (OD_{600nm} h^{-1}) and lag times (h) were extracted from growth curves by fitting a Zwietering-modified Gompertz model (**B**,**C**). Each datapoint represents a biological repeat (n= 3). Lines and bars represent the mean and error bars represent standard deviation. Significance between the treated and untreated groups was tested using a one-way ANOVA, followed by Dunnett's multiple comparisons test. All *p*-values are shown.

Supplementary References

1. Hermans, K. *et al.* Gene expression analysis of monospecies Salmonella typhimurium biofilms using differential fluorescence induction. *J. Microbiol. Methods* **84**, 467–478 (2011).
2. Bader, M. W. *et al.* Regulation of Salmonella typhimurium virulence gene expression by cationic antimicrobial peptides. *Mol. Microbiol.* **50**, 219–230 (2003).
3. Kint, G., De Coster, D., Marchal, K., Vanderleyden, J. & De Keersmaecker, S. C. The small regulatory RNA molecule MicA is involved in Salmonella enterica serovar Typhimurium biofilm formation. *BMC Microbiol.* **10**, 276 (2010).
4. Yssel, A. E. J. Perturbations in Nucleotide Biosynthesis inhibits Salmonella Biofilm Formation. (KU Leuven, 2017).
5. Dieltjens, L. *et al.* Inhibiting bacterial cooperation is an evolutionarily robust anti-biofilm strategy. *Nat. Commun.* **11**, 107 (2020).
6. Zuo, Y., De, S., Feng, Y. & Steitz, T. A. Structural Insights into Transcription Initiation from De Novo RNA Synthesis to Transitioning into Elongation. *iScience* **23**, 101445 (2020).
7. Zuo, Y., Wang, Y. & Steitz, T. A. The Mechanism of E. coli RNA Polymerase Regulation by ppGpp Is Suggested by the Structure of their Complex. *Mol. Cell* **50**, 430–436 (2013).